Unexpected shape changes of encapsulated oblate spheroids in response to equatorial traction

2008 J. Phys. A: Math. Theor. 41 495204

(http://iopscience.iop.org/1751-8121/41/49/495204)

IOP PUBLISHING JOURNAL OF PHYSICS A: MATHEMATICAL AND THEORETICAL

J. Phys. A: Math. Theor. **41** (2008) 495204 (9pp) doi:10.1088/1751-8113/41/49/495204

Unexpected shape changes of encapsulated oblate spheroids in response to equatorial traction

R A Schachar[1,6], G G Liao[2], R D Kirby[2], F Kamagar[3], J H Savoie[4], A Abolmaali[4] and G Rosensteel[5]

[1] Department of Physics, University of Texas at Arlington, Arlington, TX 76019, USA
[2] Department of Mathematics, University of Texas at Arlington, Arlington, TX 76019, USA
[3] Department of Computer Science and Engineering, University of Texas at Arlington, Arlington, TX 76019, USA
[4] Department of Civil and Environmental Engineering, University of Texas at Arlington, Arlington, TX 76019, USA
[5] Department of Physics, Tulane University, New Orleans, LA 70118, USA

E-mail: ron@2ras.com

Received 5 February 2008, in final form 5 August 2008
Published 29 October 2008
Online at stacks.iop.org/JPhysA/41/495204

Abstract

The purpose of the study was to determine the change in shape of an encapsulated spheroid associated with an increase in its circumferential equatorial diameter. Using nonlinear finite element analysis the effects of changing the spheroid's aspect ratio, the elastic modulus of its capsule and the Poisson's ratio of the encapsulated fluid were assessed. We found that when the equatorial diameter of a spheroid with an aspect ratio of $\leqslant 0.6$ was increased, the new central sagittal cross sectional profile of the oblate spheroid was no longer elliptical. The new profile had a larger minor axis, the curvature at its poles was steeper and the curvature near its equator was flatter than the original profile. The new profile referred to herein as a 'steep profile' also occurred when the major axis of a two-dimensional ellipse with an aspect ratio of $\leqslant 0.6$ was increased providing the area enclosed by the ellipse was held constant or allowed to minimally decrease. 'Steep profiles' occur in encapsulated oblate spheroids with different material properties, in two-dimensional ellipses and floating oil films. This suggests that the phenomenon may have universal implications.

PACS number: 02.30.Xx

(Some figures in this article are in colour only in the electronic version)

[6] Address for correspondence: PO Box 8669, La Jolla, CA 92038, USA.

1. Introduction

When the major axis of an encapsulated biconvex object with a long oval cross sectional profile is increased $\leqslant$5%, counterintuitively, the length of its minor axis *increases*, its central surfaces *steepen* and its peripheral surfaces flatten, i.e. the object obtains a 'steep profile'. This phenomenon has been observed in water and gel-filled oblate balloons, prolate lipid vesicles [1] and the human crystalline lens [3–7]. The 'steep profile' occurs even when the object's shape is only maintained by surface tension such as a water droplet floating freely in space [1]. To determine the basis for the 'steep profile', the shape changes induced by increasing the major axes of encapsulated spheroids and two-dimensional ellipses were analyzed.

2. Nonlinear finite element analysis (FEM)

ABAQUS (Version 6.7, ABAQUS, Inc., Pawtucket, RI, USA) was used to analyze the axisymmetric discrete FEM model of the changes in shape of fluid-filled encapsulated spheroids with aspect ratios from 0.2 to 1.0 when the equatorial diameters of the spheroids were circumferentially increased by 2%.

For the FEM mesh of the capsule and the enclosed fluid, 4-node bilinear axisymmetric quadrilateral elements and 4-node axisymmetric quadrilateral hybrid constant pressure elements were used respectively. The capsule of the spheroid had a uniform thickness of 5 μm and a Poisson's ratio $\nu = 0.47$. The elastic modulus of the capsule was varied from 0.05 MPa to 10 MPa while the elastic modulus of the enclosed fluid and its Poisson's ratio were held constant at E = 400 Pa and $\nu = 0.5$, respectively. Then the Poisson's ratio of the enclosed fluid was varied from $\nu = 0.48$ to 0.5 while the elastic modulus of the capsule was held constant at 0.5 MPa.

Standard constitutive equations for a two-dimensional axisymmetric problem were used with a mixed formulation based on displacement and pressure. The pressure variable was formulated with a Lagrange multiplier. This was done to prevent the locking phenomenon. The general discrete finite element formulation was used in which the axisymmetric solution of each element is approximated by a complete polynomial. The number of constants of the polynomial was equal to the degrees of freedom of each element. By having a completeness requirement, monotonic convergence of the elements was ensured [8]. The nonlinear problem was solved by incrementally using a piecewise linear algorithm based on the Newton–Raphson procedure [8].

For aspect ratios, $\leqslant$0.6, the length of the minor axis of the central cross sectional profile of the spheroid *increased*, the surface at its poles became *steeper* and the surface near its equator become flatter, i.e. the oblate spheroid developed a 'steep profile' (figure 1).

The 'steep profile' occurred even when the elastic modulus of the capsule was increased 200 fold from 0.05 MPa to 10 MPa and the Poisson's ratio of the enclosed fluid was decreased from $\nu = 0.5$ to 0.48 (figure 2).

3. 'Steep profiles' in two-dimensional ellipses

To test the generality of 'steep profiles', the effect of increasing the major axes of two-dimensional ellipses were analyzed. The relationship of the major axis, a, and the minor axis, b, of an ellipse in polar coordinates is given by (figure 3)

$$\frac{\rho_0^2 \cos^2(\theta)}{a^2} + \frac{\rho_0^2 \sin^2(\theta)}{b^2} = 1 \tag{1}$$

where $\rho_0 =$ the polar axis of the ellipse at baseline, $x = \rho_0 \cos(\theta)$ and $y = \rho_0 \sin(\theta)$.

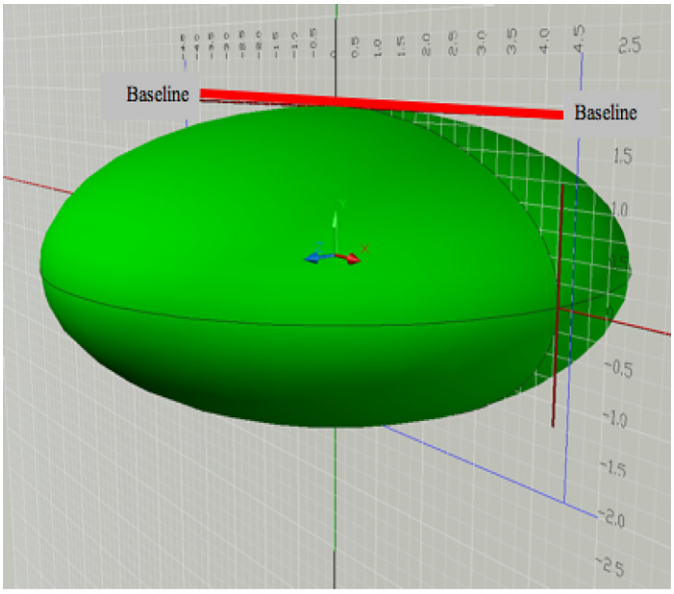

(*a*)

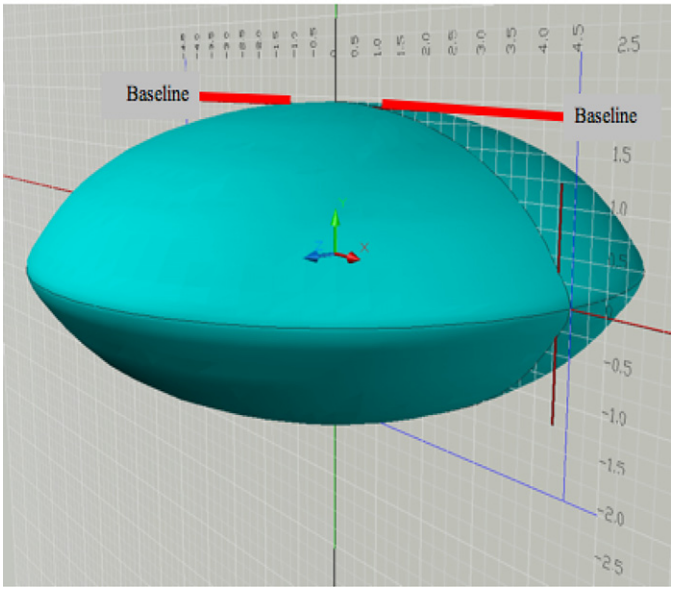

(*b*)

Figure 1. Nonlinear finite element analysis of the change in shape of an encapsulated oblate spheroid. (*a*) Baseline shape with an aspect ratio of 0.43. (*b*) 'Steep profile' induced by a small circumferential increase in the equatorial diameter. Note the increase in the minor axis.

Therefore,

$$\rho_0 = \frac{ab}{\sqrt{a^2 \sin^2(\theta) + b^2 \cos^2(\theta)}}, \qquad 0 \leqslant \theta \leqslant \frac{\pi}{2}. \tag{2}$$

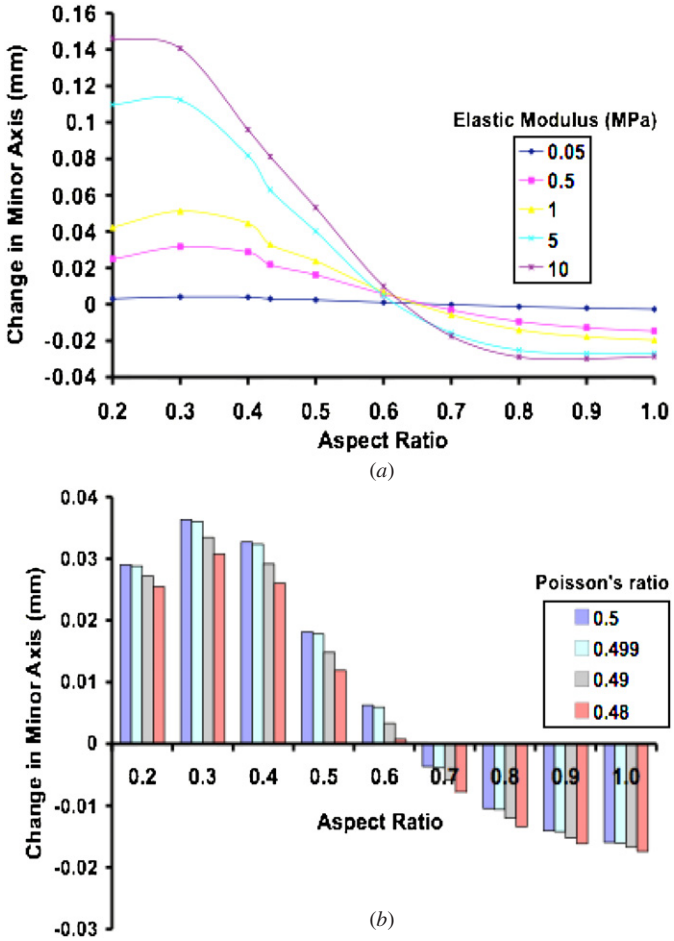

Figure 2. Nonlinear finite element analysis of the effect of (a) variation of the elastic modulus of the capsule and (b) variation of Poisson's ratio of the enclosed fluid on the change in the minor axis induced by a 2% circumferential increase in the equatorial diameter of spheroids with aspect ratios between 0.2 and 1.0. Note the increase in the minor axis of oblate spheroids with aspect ratios $\leqslant$0.6.

Using the calculus of variations, the square of the difference of the curvatures, between the baseline ellipse and the new curve were minimized. Since the change in curvature is a surrogate for the change in bending energy, this ensured that the new curve was in the minimum energy state. The polar axis of the new curve, $\rho = \rho(\theta)$, was determined from the functional

$$F(\rho, \rho_0, a, b, d) = \int_0^{\frac{\pi}{2}} [\kappa(\rho) - \kappa(\rho_0)]^2 \sqrt{\rho^2 + (\rho')^2}\, \mathrm{d}\theta \tag{3}$$

where $\kappa(\rho)$ is the curvature and is given by

$$\kappa(\rho) = \frac{|\rho^2 + 2\rho'^2 - \rho\rho''|}{(\rho^2 + \rho'^2)^{\frac{3}{2}}}. \tag{4}$$

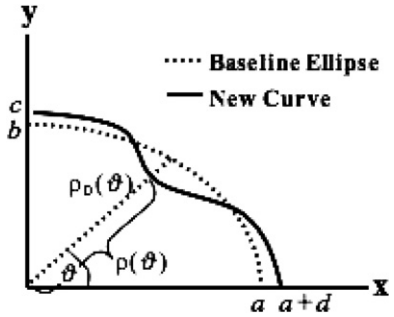

Figure 3. Polar coordinates of the ellipse and the new curve.

The problem was solved numerically, subject to the following constraints:

$$\text{Arc length} = \int_0^{\frac{\pi}{2}} \sqrt{\rho^2 + (\rho')^2}\,\mathrm{d}\theta \leqslant 1.005 \int_0^{\frac{\pi}{2}} \sqrt{\rho_0^2 + (\rho_0')^2}\,\mathrm{d}\theta. \tag{5}$$

The arc length was permitted to increase 0.5% to simulate the small stretching of the surface of biconvex objects when equatorial traction is applied

$$\text{Area under the new curve} = \int_0^{\frac{\pi}{2}} \frac{1}{2}\rho^2\,\mathrm{d}\theta = \int_0^{\frac{\pi}{2}} \frac{1}{2}\rho_0^2\,\mathrm{d}\theta, \tag{6}$$

and the boundary conditions are

$$\rho(0) = a + d \tag{7}$$

$$\rho'(0) = 0 \tag{8}$$

$$\rho'\left(\frac{\pi}{2}\right) = 0. \tag{9}$$

The interval $\left[0, \frac{\pi}{2}\right]$ was divided into n subintervals. The nodal values were denoted by $\rho_i, i = 1, 2, \ldots, n$. The cost function and the constraints were descritized by the finite difference method. This process reduced the continuous problem into a finite-dimensional nonlinear optimization problem with equality and inequality constraints. The problem was then solved with a standard optimization software program for ellipses with aspect ratios (b/a) of 0.3 to 0.8 when their major axis was increased by $d = 2\%$.

When the major axis of an ellipse, with an aspect ratio $\leqslant$0.6, was increased from 0 to 4%, the ellipse developed a 'steep profile' by undergoing three changes. As expected, the peripheral curvature decreased, i.e. it became flatter. More surprising, however, was the steepening of the curvature at the pole and the increase in the length of the minor axis (figure 4).

For a given increase in the major axis of the baseline ellipse, the shape of the 'steep profile' was enhanced as the aspect ratio of the baseline ellipse was decreased from 0.6 to 0.3. In response to a specific increase in the major axis of the ellipse, the change in curvature and length of the minor axis occurred more efficiently when the aspect ratio was $\leqslant$0.6 (figure 5). The 'steep profile' occurred even when the area under the curve was decreased by approximately 1% and the arc length of the ellipse was held constant.

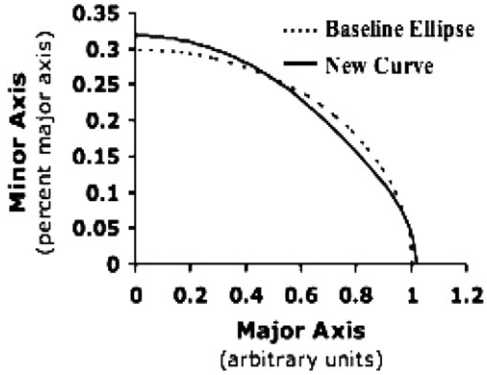

Figure 4. The change in shape of an ellipse, baseline aspect ratio = 0.3, in response to a 2% increase in its major axis, when the area enclosed by the curve remains constant and the arc length is permitted to increase 0.5%.

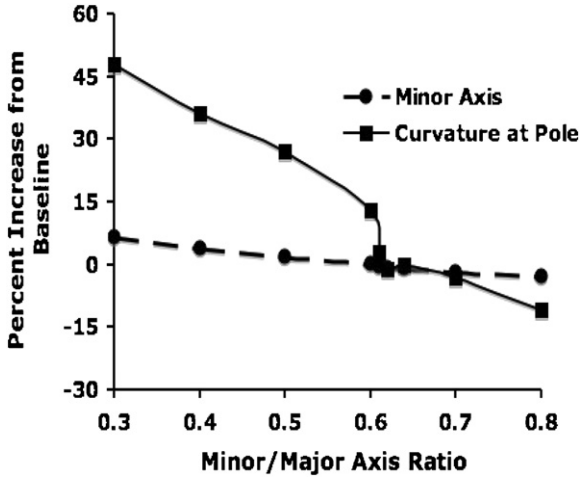

Figure 5. The effect of the baseline aspect ratio of an ellipse on the change in the length of the minor axis and curvature at the pole, when the major axis of the ellipse was increased 2%. The area enclosed by the ellipse was held constant and the arc length was permitted to increase $\leqslant$0.5%.

4. Floating oil film

To qualitatively compare these predictions with experimental data, the 180° meridian of a circular mineral oil film, floating on water, was increased by electromechanically moving wires apart in 0.500 mm steps for 14 steps and then in 0.025 mm steps until the oil film separated (figure 6). Each bilateral step was separated by at least a one-minute interval to ensure that each new shape of the oil film was in equilibrium. After each bilateral step, a digital photograph of the upper surface of the oil film was recorded and analyzed. An optically clear, acrylic supporting box, measuring 8 cm by 8 cm by 3 cm, was placed on a white piece of glass. A Polaroid sheet was placed on top of this box. A second acrylic box, with an open top, 10 cm by 6 cm by 5 cm, was stacked on top of the Polaroid sheet. Distilled water was used to fill the upper acrylic box. Using a digital micropipette (Socorex [Lausanne, Switzerland]

Figure 6. Experimental set up. A circular film of mineral oil was floated on water. Metal pins extended only into the oil film and not into the water below. The pins were connected to electronic micrometers to apply traction in the 180° meridian.

Calibra 822.1000), a 250 $\mu l \pm 3.4$ μl circular film of clear mineral oil was placed on the water's surface. A fiber optic light illuminated the supporting acrylic box from below. A digital camera (EOS D30 with a 100 mm Macro lens, Canon, Lake Success, NY, USA) was centered over the circular oil film and mounted on the optical bench. A non-moving steel wire of 1.0 mm diameter was attached to the optical bench extended onto the surface of the water at the same level as the floating oil film and served as a non-varying dimensional reference in all photographs. Two steel wires with blunt ends, measuring 2.5 cm long and 1.1 mm in diameter, were each attached to horizontal steel rods, using molding clay. Each wire made a 110° angle with the bottom of the steel rods. The steel rods were each fixed to electronically controllable vertical stages, which were mounted on electronically controlled horizontal stages that were attached to the optical bench. In this way both the horizontal and vertical position of the wires were electronically controlled (figure 6). The wires were placed 180° apart into the circular oil film so that each was very close to the center of the oil film. It was visually and photographically confirmed that the tips of the wires applying the traction extended only into the oil film and **not** into the water below.

Using image software (ImageJ, National Institutes of Health, USA), the major axis, minor axis and area of the oil film were measured. The best fitting parabola with a 4 mm arc length centered on the 90° meridian of the perimeter of the oil film was used to calculate the radius of curvature. Initially, as the 180° meridian of the circular oil film was increased, the circular oil film became elliptical with its major axis in the tractional meridian. As the major axis of the elliptical oil film was increased, its eccentricity increased (figures 7(*a*) and 7(*b*)). Once the aspect ratio of the oil film was equal to 0.6 (figure 7(*c*)), a small increase in the major axis caused the oil film to develop a 'steep profile' (figure 7(*d*)). With additional traction in the major axis, the shape of the 'steep profile' became more pronounced until its aspect ratio was approximately 0.50, then the oil film separated in two unequal circular films centered on the wires (figures 7(*e*) and 7(*f*)). The efficiency of the traction for deforming the shape of the oil film was significantly greater when the aspect ratio of the oil film was <0.6 (figure 8). Furthermore, for a 2% increase in the major axis of the oil film, the percent change in the

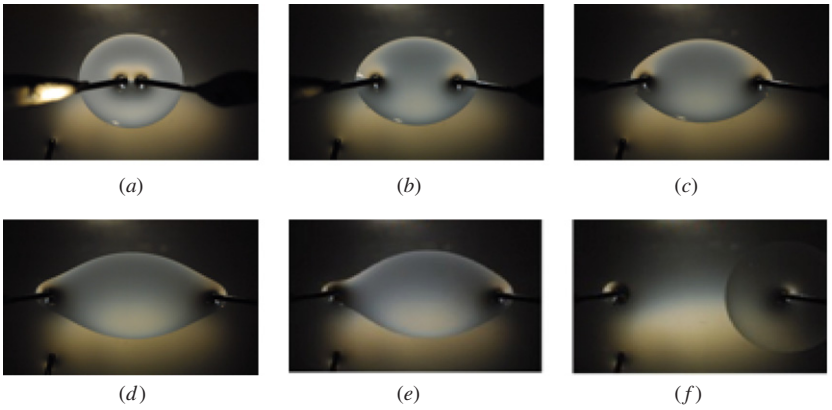

Figure 7. Photographs of the oil film during progressively increasing traction in the 180° meridian (*a*) at baseline, (*b*) elliptical, minor to major axis ratio = 0.78, (*c*) minor axis to major axis ratio = 0.6 (long oval), (*d*) 'steep profile', (*e*) beginning to separate, (*f*) completely separates into two unequal circular films.

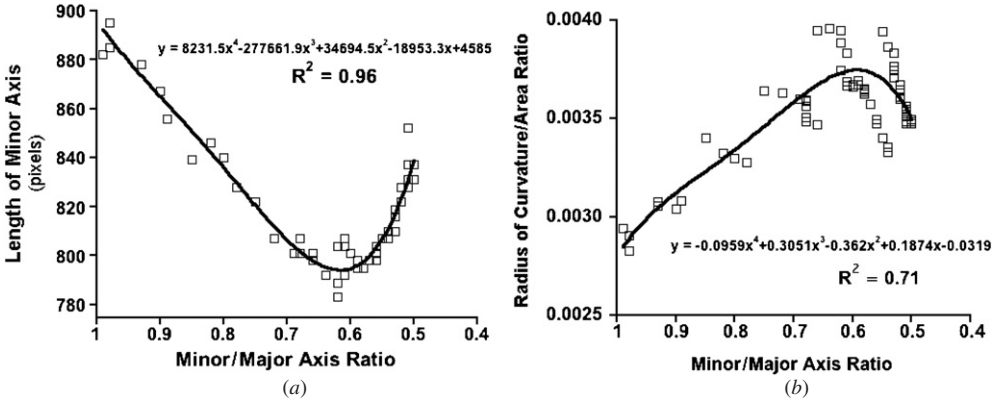

Figure 8. (*a*) Length of the minor axis of the oil film versus the aspect ratio of the oil film. (*b*) Radius of curvature to area ratio versus the aspect ratio of the oil film in response to a 2% increase in its major axis.

oil film's minor axis versus its aspect ratio was in good agreement with the analysis of the ellipse.

5. Conclusion

We have shown that an encapsulated oblate spheroid and a two-dimensional ellipse, with aspect ratios $\leqslant 0.6$, develop 'steep profiles' in response to a small increase in their major axis provided that the volume of the oblate spheroid and the area enclosed by the ellipse minimally change. 'Steep profiles' are seen in biconvex objects with a range of material properties including floating oil films whose shape is maintained only by surface tension. The human lens is an encapsulated oblate spheroid with a Poisson's ratio $\nu = 0.5$ and an aspect ratio $\leqslant 0.6$ [9–11]. During accommodation, when the eye focuses for near vision, the central thickness

of the lens increases and its central surfaces steepen while its peripheral surfaces flatten, i.e. the lens develops a 'steep profile'. The 'steep profile' accounts for the increase in central optical power and the negative shift in spherical aberration that occurs during accommodation [12–17]. Minimization of the difference in curvature, a surrogate for bending energy, explains the occurrence of the 'steep profile' (figures 1(*b*), 4 and 7(*d*)).

Acknowledgments

The authors wish to thank Professor Zdzislaw E Musielak and Professor Truman D Black of the Department of Physics, University of Texas at Arlington, Arlington, Texas for their constructive inputs and wish to dedicate this work in memory of Professor Tseng (Leo) Huang (1925–2006) of the Department of Civil and Environmental Engineering.

References

[1] Schachar R A and Fygenson D K 2007 *Br. J. Ophthalmol.* **91** 1698
[2] Schachar R A 2004 *Invest. Ophthalmol. Vis. Sci.* **45** 2691
[3] Abolmaali A, Schachar R A and Le T 2007 *Comput. Methods Programs Biomed.* **85** 77
[4] Chien C H, Huang T and Schachar R A 2006 *J. Biomech.* **39** 672
[5] Belaidi A and Pierscionek B K 2007 *J. Vis.* **7** 1
[6] Chien C H, Huang T and Schachar R A 2003 *Compr. Ther.* **29** 167
[7] Schachar R A, Pierscionek B K, Abolmaali A and Le T 2007 *Br. J. Ophthalmol.* **91** 812
[8] Bathe K J 1996 *Finite Element Procedure* (Englewood Cliffs, NJ: Prentice-Hall)
[9] Mann I 1969 *The Development of the Human Eye* (New York, NY: Grune Stratton)
[10] Kuszak J R, Zoltoski R K and Sivertson C 2004 *Exp. Eye Res.* **78** 673
[11] Schachar R A 2005 *J. Anat.* **206** 575
[12] Young T 1801 *Phil. trans. R. Soc.* **92** 23
[13] Tscherning M 1904 *Physiological Optics* 2nd edn (Philadlphia, PA: The Keystone)
[14] Li Y, Chalita M R and Huang D 2005 *Invest. Ophthalmol. Vis. Sci.* **46** 2554 (E-Abstract)
[15] Schachar R A, Tell C, Cudmore D P, Liebmann J M, Black T D and Ritch R 1996 *Am J. Physiol. Regul. Integr. Comp. Physiol.* **271** (3Pt 2) R670
[16] Schachar R A and Kamangar F 2006 *Eye* **20** 226
[17] Schachar R A and Koivula A 2008 *Br. J. Ophthalmol.* **92** 348